



Mechanical properties of squeeze-cast Al–7Si–0.3Mg alloys with Sc-modified Fe-rich intermetallic compounds

Kittisak Chanyathunyaroj, Ussadawut Patakham, Sindo Kou,
Chaowalit Limmaneevichitr*

Received: 21 January 2017 / Revised: 12 March 2017 / Accepted: 26 September 2017 / Published online: 25 October 2017
© The Nonferrous Metals Society of China and Springer-Verlag GmbH Germany 2017

Abstract Iron (Fe) has a low solid solubility in aluminum (Al), and it usually forms Fe-rich intermetallic compounds. Scandium (Sc) is an element that can act as a grain refiner, modify the eutectic silicon and change the morphology of Fe-rich intermetallic compounds at the same time. The present work was conducted to study the effect of Sc on the mechanical properties of Al–7Si–0.3Mg. The alloy was prepared by squeeze casting at two levels of Fe (0.2 and 0.4 wt%) and three levels of Sc (0 wt%, 0.2 wt% and 0.4 wt%). Sc is found to increase the mechanical properties of the alloy, including its hardness, yield strength and ultimate tensile strength. At 0.2 wt% Fe, adding Sc increases the strength while maintaining good elongation. At 0.4 wt% Fe, adding Sc increases the strength but decreases the elongation slightly. The distributions and morphologies of intermetallic compounds and eutectic silicon affect the elongation. Both Fe-rich intermetallic compounds and Sc-rich intermetallic compounds act as crack initiation sites. The 0.2 wt% Fe + 0.2 wt% Sc alloy has the lowest amount of these intermetallic compounds, and eutectic silicon is small and fibrous. So, it has the highest elongation.

Keywords Sc-rich intermetallic compounds; Scandium; Al–Si–Mg alloy; Mechanical properties

1 Introduction

Iron (Fe) is a common impurity and difficult to remove in aluminum–silicon alloys (Al–Si alloys). In practice, Fe contamination is common in recycling of Al scrap. Fe also leads to the formation of porosity in Al–Si alloys [1]. Fe content, cooling rate and alloy composition are known to be associated with the formation of Fe-rich intermetallic compounds. The β -Al₅FeSi phase is found at low cooling rates [2, 3]. The Fe content of an aluminum alloy affects the formation of Fe-rich intermetallic compounds. Changing Fe content will change the formation of Fe-rich intermetallic compounds [4]. If Fe content is high, the β -Al₅FeSi phase will have a good chance to form [5]. The morphology of Fe-rich intermetallic compounds can significantly affect both the tensile strength and ductility of Al–Si alloys [6, 7]. The β -Al₅FeSi phase affects mechanical properties, particularly ductility. If the size of the β platelets decreases, the mechanical properties increase, including tensile strength and ductility increase [8, 9]. Previous studies tried to change the β -Al₅FeSi phase into other phases by adding elements such as manganese (Mn), chromium (Cr) and beryllium (Be). Adding Mn caused α -Al(Mn,Fe)Si to form. Adding Cr and Mn caused α -Al(Mn,Cr,Fe)Si to form in a granular shape. And adding Be caused (Be–Fe)-BeSiFe₂Al₈ to form [7, 10–15].

Modifying eutectic silicon and refining grain size can increase the mechanical properties of hypoeutectic Al–Si alloys. Normally, adding strontium (Sr) is a way to modify the eutectic silicon in the hypoeutectic Al–Si alloy. Adding

K. Chanyathunyaroj, C. Limmaneevichitr*
Production Engineering Department, Faculty of Engineering,
King Mongkut's University of Technology Thonburi,
Bangkok 10140, Thailand
e-mail: chaowalit.lim@mail.kmutt.ac.th

U. Patakham
National Metal and Materials Technology Center, National
Science and Technology Development Agency, Khlong Nueng,
Pathumthani 12120, Thailand

S. Kou
Department of Materials Science and Engineering, University of
Wisconsin-Madison, Madison, WI 53706, USA

0.02 wt% Sr can make the modification of eutectic silicon completely [16–18]. In grain refinement, Al–Ti or Al–Ti–B is added into the hypoeutectic Al–Si alloy [19, 20]. Scandium (Sc) has much beneficial effect on aluminum alloys [21, 22]. Adding Sc in Al–Si alloys as a minor alloying element can both refine the grain size [23] and modify the eutectic silicon at the same time [24], though, less effective in grain refining than Al–Ti–B and in modifying the eutectic silicon than Sr [25, 26]. In addition, Sc can change Fe-rich intermetallic compounds into Sc-rich intermetallic compounds (Chinese script like and skeleton like) [27, 28]. Therefore, to increase mechanical properties, Sc is a better choice because it can modify eutectic silicon, act as a grain refiner and also change the morphology of Fe-rich intermetallic compounds.

In squeeze casting of aluminum alloys, solidification under high pressure is promoted by applying force to liquid aluminum in a permanent mold, which improves the mechanical properties of Al–Si alloys [29]. Furthermore, this process decreases porosity because of the compressed liquid metal in high-pressure state during solidification. Under high pressure, shrinkage can be filled and entrapped gases can remain in the solution [30].

To successfully modify eutectic silicon and to grain refine Al–Si–Mg casting alloys, the minimum addition amount of Sc is 0.4 wt% [23, 26]. The liquid aluminum is capable of dissolving iron from unprotected steel tools in production process [6]. In general, it is undesirable to have iron in aluminum alloys. If the iron contamination is unavoidable, it is necessary to investigate the effect of iron contamination in Sc-modified Al–Si–Mg. Although it has been attempted to determine the effect of Sc addition on Fe-bearing phases and tensile properties, the Fe and Sc contents were very low and Sr was also added to modify the eutectic silicon [31]. The present work was undertaken to identify the mechanical properties of Al–7Si–0.3Mg whose Fe-rich intermetallic compounds were changed into Sc-rich ones (Chinese script like and skeleton like) by adding Sc. Squeeze casting was chosen to reduce the adverse effect of porosity on the mechanical properties.

2 Experimental

Al–7Si–0.3Mg (A356) aluminum alloy was the base of the alloys investigated in the present studies. Al–7Si–0.3Mg alloys were prepared from pure aluminum to minimize possible contamination by trace elements. Six Al–7Si–0.3Mg alloys with about 3500 g in total quantity were prepared by using master alloys of Al–2 wt% Sc and Al–10 wt% Fe to adjust their chemical compositions to 0.2Fe, 0.2Fe + 0.2Sc, 0.2Fe + 0.4Sc, 0.4Fe, 0.4Fe + 0.2Sc and 0.4Fe + 0.4Sc. These compositions were selected based on

a previous work [27]. Each aluminum alloy was melted in a silicon carbide crucible using a 12-kW induction furnace. The chemical compositions of the alloys were determined by emission spectrometry, as listed in Table 1. The melt was poured into an ingot tray, which was then prepared for squeeze casting by dividing into smaller ingots with 750 grams each.

Squeeze casting was used to study the mechanical properties. The size of mold was 68 mm in inner diameter and 70 mm in height [32]. The mold was made from tool steel and preheated to 250 °C before casting. The 750-g ingot was remelted and heated to 720 °C, and the melt was degassed by purging argon gas (Ar) through a stainless steel tube (6-mm inside diameter) coated with zircon on the outside and immersed in the melt. In each case, the degassing time was 1 min before pouring into the mold. The squeezing force was adjusted to 75 MPa with the help of a load cell. The squeezing time was 1 min. After casting, the rectangular blocks were prepared by a wire-cut process for microstructural examination, hardness testing and tensile testing, as illustrated in Fig. 1. The rectangular blocks (5 mm × 10 mm × 70 mm) were cut along the radial direction at 15 to 25 mm.

The tensile specimens were prepared from the rectangular blocks by wire-cut electrical discharge (ED) machine. The dimensions of the rectangular tensile specimen are shown in Fig. 2, following ASTM B557 M. The dimensions at gage length position were 25 mm in length, 6 mm in width and 5 mm in thickness. The stretching rate for tensile testing was 1 mm·min^{−1}. A Lloyd LR 50 K machine was used for tensile testing. The yield strength was determined based on 0.2% offset.

The microstructure and hardness were examined inside the gauge length of tensile specimens. The samples for microstructural examination were prepared by standard metallographic procedures on optical microscope (Olympus GX51F). They were etched with a 0.5% HF–water solution. A Brinell 2.5-mm ball was used for the hardness testing. A Hitachi model S-3400 N scanning electron microscope (SEM) was used for analyzing the intermetallic compounds and fracture surfaces of tensile-tested specimens.

Table 1 Chemical compositions of alloys (wt%)

Alloys	Si	Mg	Sc	Fe	P	Al
0.2Fe	7.06	0.31	< 0.001	0.21	0.0011	Bal.
0.2Fe + 0.2Sc	7.06	0.31	0.210	0.21	0.0010	Bal.
0.2Fe + 0.4Sc	7.12	0.31	0.410	0.21	0.0009	Bal.
0.4Fe	7.10	0.33	< 0.001	0.40	0.0011	Bal.
0.4Fe + 0.2Sc	7.01	0.30	0.210	0.42	0.0012	Bal.
0.4Fe + 0.4Sc	7.15	0.32	0.410	0.40	0.0009	Bal.

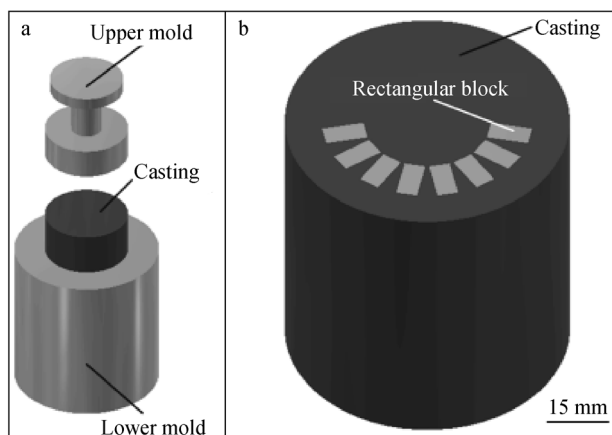


Fig. 1 Schematic illustration of squeeze casting: **a** squeeze mold and **b** area for preparing tensile specimen

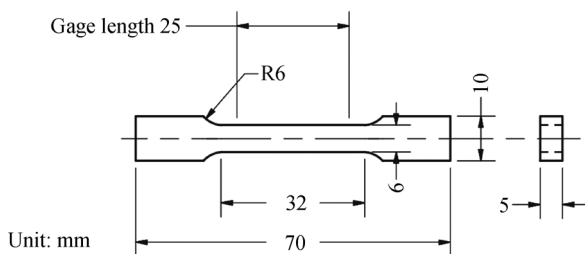


Fig. 2 Dimensions of tensile specimen followed by ASTM B557 M [30]

3 Results and discussion

3.1 Effect of scandium on microstructure

Figure 3 shows OM images of tensile specimens. No porosity is visible. The eutectic silicon of the 0.2Fe alloy (Fig. 3a) is the coarsest, followed by that of 0.4Fe alloy (Fig. 3b). Adding Sc changes the eutectic silicon from a plate-like structure with sharp edges to one more fibrous, consistent with previous studies [24–26]. Figure 3c–f shows the morphology of the eutectic silicon in 0.2Fe + 0.2Sc, 0.2Fe + 0.4Sc, 0.4Fe + 0.2Sc and 0.4Fe + 0.4Sc alloys, which is finer than that in Sc-free alloys (0.2Fe and 0.4Fe alloys). In previous work, adding Sc changed the morphology of Fe-rich intermetallic compounds by forming Sc-rich intermetallic compounds. The previous work classified the Sc-rich intermetallic compounds into four types of phases [27]. From the available Al–Si–Sc ternary phase diagram [33, 34], one of the existence of ternary phases should be AlSi_2Sc_2 . However, there are other complex phases (consisting of Al, Mg, Si, Sc and Fe) that may not be simply explained because of limited data of those phase diagrams. In this experiment, the Sc-rich intermetallic compounds were used to call these four types of phases. Figure 3 shows that the addition of Sc

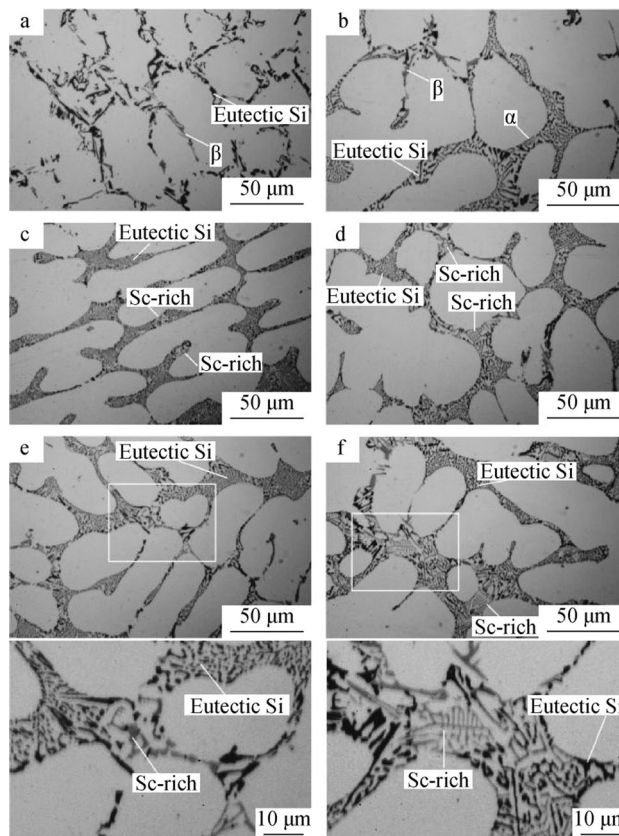


Fig. 3 OM images of tensile specimens: **a** 0.2Fe, **b** 0.4Fe, **c** 0.2Fe + 0.2Sc, **d** 0.4Fe + 0.2Sc, **e** 0.2Fe + 0.4Sc and **f** 0.4Fe + 0.4Sc

changes the morphology of the Fe-rich intermetallic compounds (α phase and β phase) into Sc-rich intermetallic compounds. The morphology of intermetallic compounds is not clear in optical micrographs. The SEM-backscattered electron (BSE) was used to analyze the morphology of intermetallic compounds. Figure 4 shows SEM-BSE images of tensile specimens. Figure 4a, b shows Fe-rich intermetallic compounds (α phase and β phase) in 0.2Fe and 0.4Fe alloys. Almost all Fe-rich intermetallic compounds form into platelet-like phase (β phase). The amount and size of the β phase in 0.4Fe alloy are greater than those of 0.2Fe alloy. Figure 4c–f shows the morphology of intermetallic compounds in 0.2Fe + 0.2Sc, 0.2Fe + 0.4Sc, 0.4Fe + 0.2Sc and 0.4Fe + 0.4Sc alloys, which are mostly Sc-rich intermetallic compounds, showing that the addition of Sc changes Fe-rich intermetallic compounds (α phase and β phase) into Sc-rich intermetallic compounds. The shape of Sc-rich intermetallic compounds is rounder than that of β phase. Some Fe-rich intermetallic compounds remain as β phase. The amount of β Fe-rich intermetallic compound and Sc-rich intermetallic compounds in 0.4Fe alloys with Sc (0.4Fe + 0.2Sc and 0.4Fe + 0.4Sc alloys) is higher than that in 0.2Fe alloys with Sc (0.2Fe + 0.2Sc

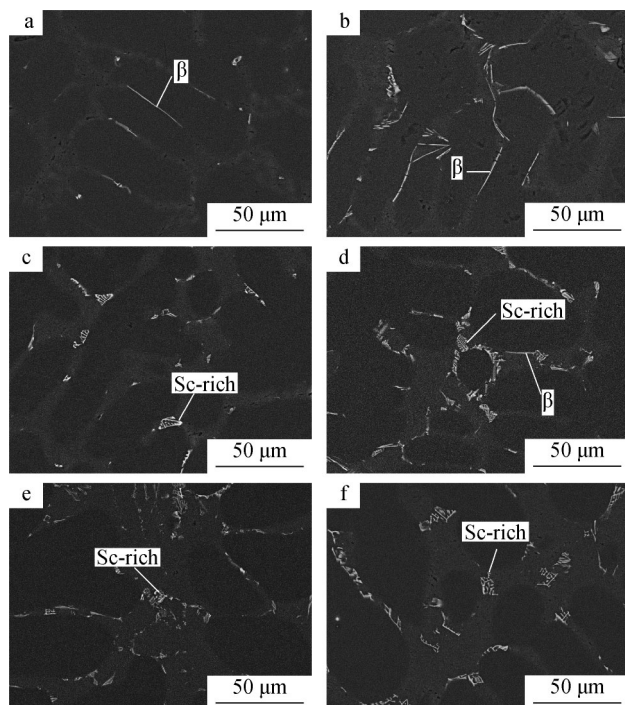


Fig. 4 SEM-BSE images of tensile specimens: **a** 0.2Fe, **b** 0.4Fe, **c** 0.2Fe + 0.2Sc, **d** 0.4Fe + 0.2Sc, **e** 0.2Fe + 0.4Sc and **f** 0.4Fe + 0.4Sc

and 0.2Fe + 0.4Sc alloys). Adding Sc can modify the eutectic silicon and change the Fe-rich intermetallic compounds at the same time. This benefit of Sc should increase the mechanical properties of Al–Si–Mg alloy.

3.2 Effect of scandium on mechanical properties

3.2.1 Effect of scandium on hardness

The results of Brinell hardness are shown in Fig. 5 and Table 2. They show the means of 15 sets of results per alloy, the error bars and standard deviations (in parentheses). In the as-squeeze-cast condition, the hardness of Sc-free alloys (0.2Fe and 0.4Fe alloys) is HB 56–HB 58 approximately. The hardness of 0.4Fe alloy is slightly higher than that of 0.2Fe alloy. The addition of Sc significantly increases the hardness. With the addition of 0.2 wt% Sc, the hardness of 0.2Fe + 0.2Sc and 0.4Fe + 0.2Sc alloys is HB 67 approximately. Increasing Sc to 0.4 wt % (0.2Fe + 0.4Sc and 0.4Fe + 0.4Sc alloys) increases the hardness to HB 69.

3.2.2 Effect of scandium on tensile properties and elongation

The results of tensile tests are shown in Fig. 6 and Table 2. The stretching rate was 1 mm·min⁻¹. The results are based

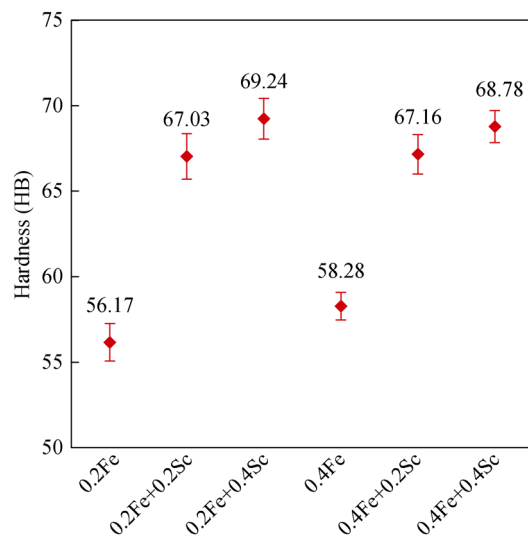


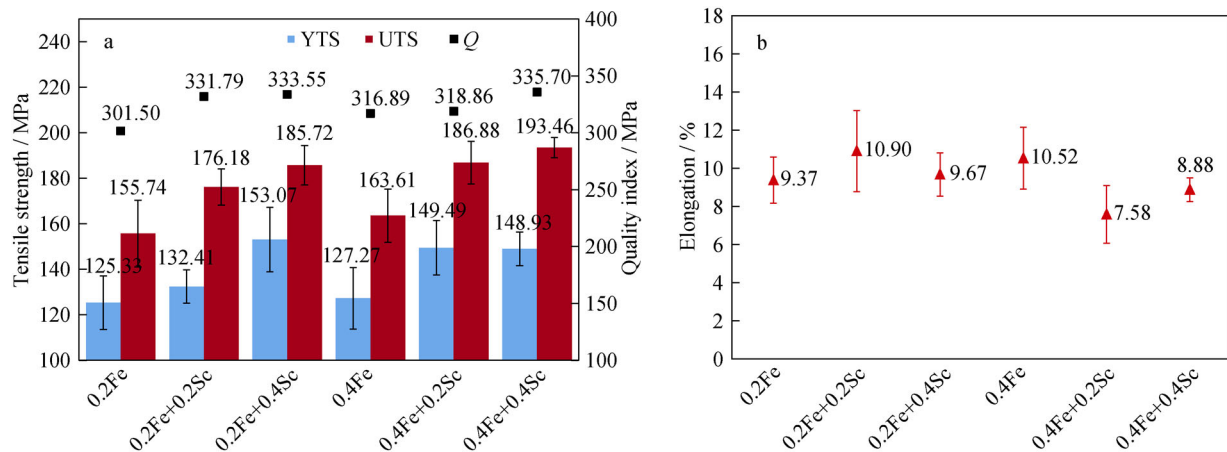
Fig. 5 Brinell hardness result (error bars indicating standard deviations)

on twelve tensile tests per alloy, with the error bars and brackets showing standard deviations. The difference in Fe content does not affect the yield strength (YTS) and ultimate tensile strength (UTS). The Sc-free alloys (0.2Fe and 0.4Fe alloys) have approximately 125-MPa YTS and 160-MPa UTS. The addition of Sc increases YTS and UTS. The 0.2Fe + 0.4Sc and 0.4Fe + 0.4Sc alloys have approximately 150-MPa YTS and 190-MPa UTS. The elongation results are shown in Fig. 6b and Table 2. Adding Sc maintains good elongation of 0.2Fe alloys, i.e., 0.2Fe + 0.2Sc and 0.2Fe + 0.4Sc. However, the elongation of 0.4Fe alloys with Sc, i.e., 0.4Fe + 0.2Sc and 0.4Fe + 0.4Sc, decreases slightly. The 0.2Fe + 0.2Sc alloy has the highest elongation. To better evaluate the tensile properties, a quality index (Q) was calculated using both tensile strength and elongation. The quality index (Q) is defined as $Q = \text{UTS} + a \lg(\text{elongation})$, where a is 150 for Al–7Si–0.3Mg alloy [35]. Since the quality index combines both strength and ductility, it is much more practical to use than either tensile strength or elongation alone. Figure 6a and Table 2 show the quality index of Al–7Si–0.3Mg alloys with and without Sc. It is found that the addition of Sc can increase the quality index by approximately 20–30 MPa.

In summary, increasing Fe from 0.2 wt% to 0.4 wt% does not affect the mechanical properties. Adding Sc can result in similar tensile results found in Al–Si-based alloys with Mn addition by Seifeddine et al. [15]. In the as-squeeze-cast condition, the addition of Sc increases the hardness by approximately HB 10. Furthermore, adding Sc increases both YTS and UTS of Al–7Si–0.3Mg by approximately 20 MPa. In 0.2Fe alloys with Sc (0.2Fe + 0.2Sc and 0.2Fe + 0.4Sc), the addition of Sc

Table 2 Mechanical properties results of alloys (numbers inside parentheses indicating standard deviations)

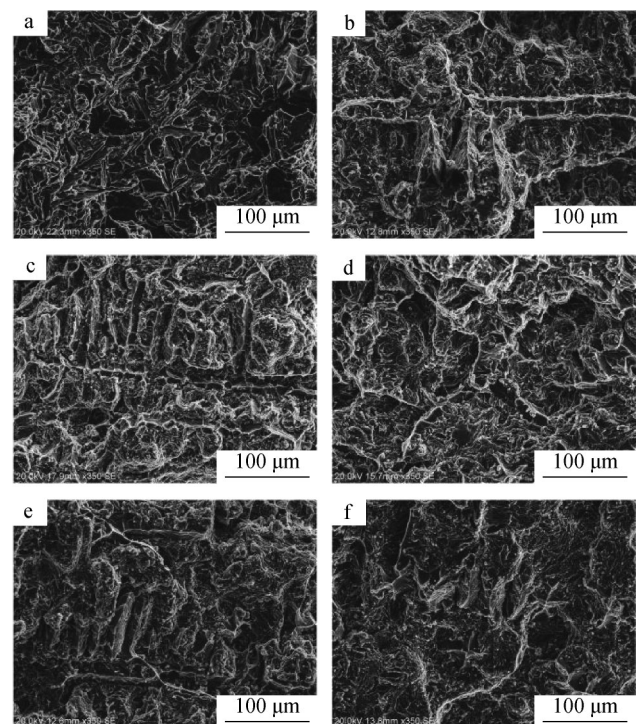
Alloys	YTS/MPa	UTS/MPa	Elongation/%	Hardness (HB)	Q/MPa
0.2Fe	125.33 (11.75)	155.74 (4.64)	9.37 (1.21)	56.17 (1.10)	301.50
0.2Fe + 0.2Sc	132.41 (7.32)	176.18 (7.98)	10.90 (2.12)	67.03 (1.33)	331.79
0.2Fe + 0.4Sc	153.07 (14.14)	185.72 (8.62)	9.67 (1.13)	69.24 (1.19)	333.55
0.4Fe	127.27 (13.49)	163.61 (11.66)	10.52 (1.62)	58.28 (0.80)	316.89
0.4Fe + 0.2Sc	149.49 (12.02)	186.88 (9.31)	7.58 (1.51)	67.16 (1.15)	318.86
0.4Fe + 0.4Sc	148.93 (7.38)	193.46 (4.47)	8.88 (0.62)	68.78 (0.94)	335.70

**Fig. 6** Tensile testing results of alloys: **a** YTS, UTS and quality index (*Q*); **b** elongation (error bars indicating standard deviations)

increases tensile strength while maintaining good elongation. With the amount of Fe increasing to 0.4 wt% (0.4Fe + 0.2Sc and 0.4Fe + 0.4Sc), the addition of Sc increases tensile strength while decreases the elongation slightly. The modification of eutectic silicon can increase the mechanical properties. Addition of Sc increases the quality index similar to the addition of other modifiers (Sr and La) [36, 37]. It has been reported that the addition of Sc reduces interdendritic shrinkage. Thus, adding Sc into Al-7Si-0.6Mg alloy can significantly improve the ductility [31]. Samples in this study were prepared by squeeze casting; thus, porosity and interdendritic shrinkages were minimized. Thus, addition of Sc does not significantly improve the elongation in this experiment.

3.3 Fracture morphology

Figure 7 shows SEM images of fracture surfaces of tensile-tested specimens. As can be seen, the fracture surfaces of all alloys in this work show a mixed quasi-cleavage and dimple morphology. A similar morphology was observed in A356 alloy by Jiang et al. [38]. It shows that the fracture surfaces of all alloys in this work display a clearly brittle fracture. The fracture paths tend to pass through the eutectic silicon. However, the mechanism of fracture is affected by the Sc content, as shown in Figs. 8–10.

**Fig. 7** SEM images of fractography of samples: **a** 0.2Fe, **b** 0.4Fe, **c** 0.2Fe + 0.2Sc, **d** 0.4Fe + 0.2Sc, **e** 0.2Fe + 0.4Sc and **f** 0.4Fe + 0.4Sc

Figures 8 and 9 show optical micrographs of tensile-tested specimens near fracture surface. The fracture of Sc-free alloys (0.2Fe and 0.4Fe alloys) appears to initiate from Fe-rich intermetallic compound (β phase) or eutectic silicon, as indicated by black ovals in Figs. 8a and 9a. The black ovals show secondary fracture in the interdendritic eutectic region, which should be the initiation site of the fracture. Fracture initiates from interdendritic eutectic region and sometimes from Fe-rich intermetallic compound (β phase). The fracture path runs along the interdendritic eutectic region. It depends on the sizes and morphologies of Fe-rich intermetallic compound and eutectic silicon. Eutectic silicon is plate like and large. The β Fe-rich intermetallic compound is also platelet like in shape. For these two reasons, fracture initiates and propagates along the interdendritic eutectic region.

Figure 8b, c shows that in 0.2Fe alloys with Sc (0.2Fe + 0.2Sc and 0.2Fe + 0.4Sc alloys), the fracture path can cut through dendrites (α -primary aluminum) in some region. The white arrow points to the remaining of a fractured dendrite. These alloys have less secondary fracture than the other alloys. As shown in Fig. 4, these alloys have a small amount of Sc-rich intermetallic compounds and the morphology of eutectic silicon is small and fibrous.

Thus, it is difficult for them to be effective crack initiation sites. This is why 0.2Fe alloys with Sc have high tensile strength and maintain a good elongation.

Figure 9b, c shows the fracture of 0.4Fe alloys with Sc (0.4Fe + 0.2Sc and 0.4Fe + 0.4Sc alloys). The black ovals show the secondary fracture in interdendritic eutectic that should be the initiation site of the fracture. The secondary fracture initiates from Sc-rich intermetallic compounds. The fracture of 0.4Fe alloys with Sc is different from that of 0.2Fe alloys with Sc. The fracture of 0.4Fe alloys with Sc runs along interdendritic eutectic region. The fracture can run through the group of eutectic silicon. The morphology of eutectic silicon is small and fibrous, but there are a lot of Fe-rich and Sc-rich intermetallic compounds inside the interdendritic eutectic region. These intermetallic compounds are crack initiation sites. The fracture can run from one intermetallic compound to another one, instead of through dendrite (α -primary aluminum). These make the fractures run through the cross section of the tensile specimen easier. Thus, the elongation of 0.4Fe alloys with Sc is lower than the other alloys.

SEM-BSE was used to analyze the fracture for further understanding. Figure 10 shows SEM images near the fracture surface of 0.4Fe, 0.2Fe + 0.2Sc and

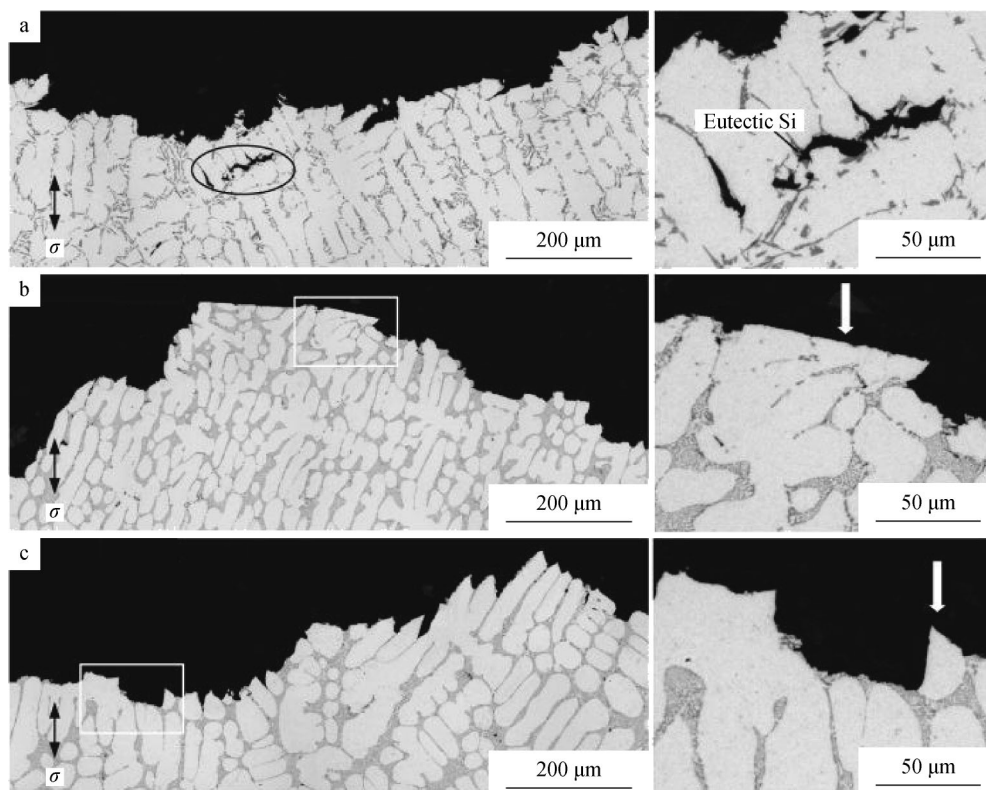


Fig. 8 OM images and corresponding enlarged images of fracture of 0.2 wt% Fe alloys: **a** 0.2Fe, **b** 0.2Fe + 0.2Sc and **c** 0.2Fe + 0.4Sc (black ellipse showing secondary fracture in interdendritic eutectic region; white arrows pointing to the remaining of dendrite; double-headed arrows and σ indicating tensile testing direction and tensile stress, respectively)

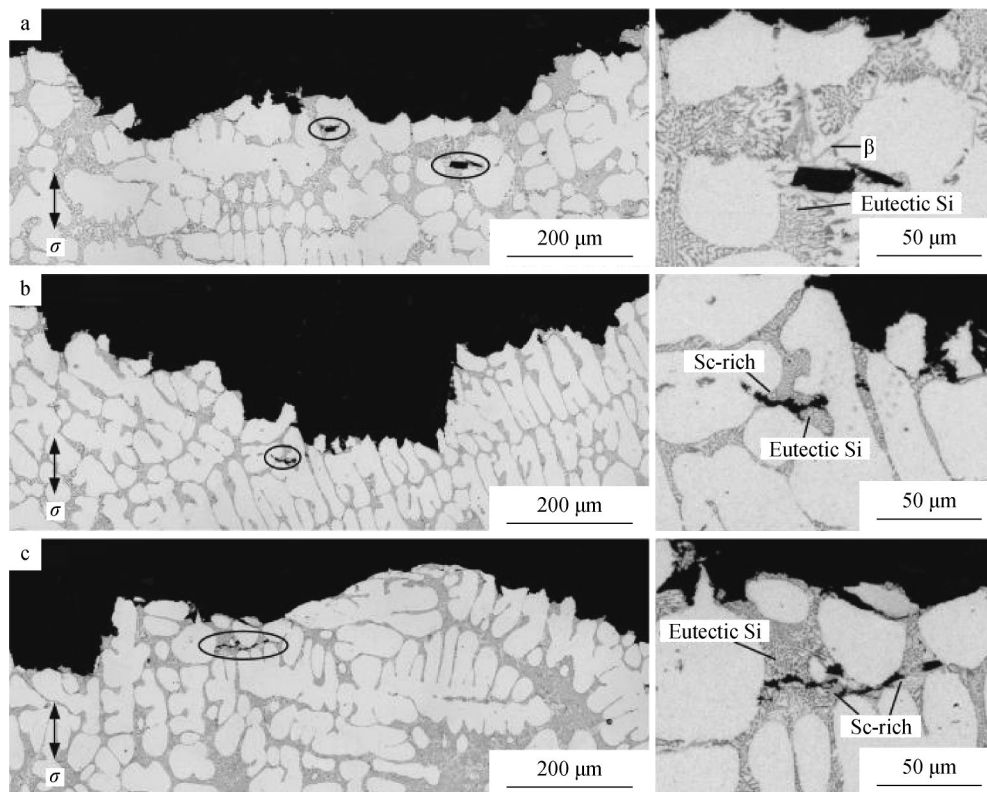


Fig. 9 OM images and corresponding enlarged images of fracture of 0.4 wt% Fe alloys: **a** 0.4Fe, **b** 0.4Fe + 0.2Sc and **c** 0.4Fe + 0.4Sc (black ellipses showing secondary fracture in interdendritic eutectic region; double-headed arrows and σ indicating tensile testing direction and tensile stress, respectively)

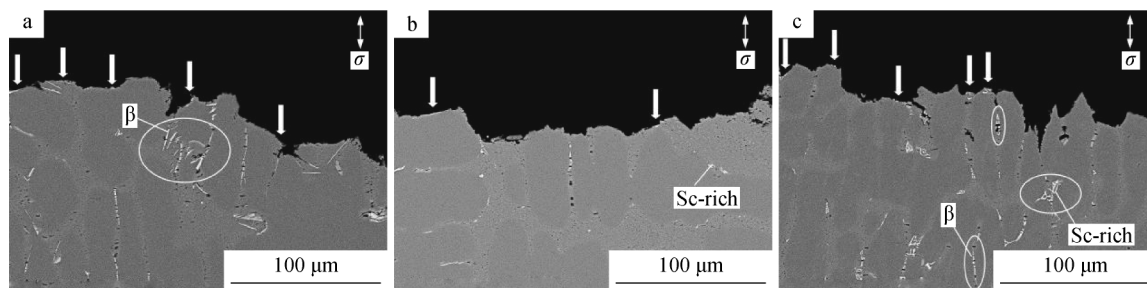


Fig. 10 SEM-backscattered electron images of fracture of **a** Sc-free alloy (0.4Fe), **b** low-Fe alloy with Sc (0.2Fe + 0.2Sc) and **c** high-Fe alloy with Sc (0.4Fe + 0.2Sc) (white arrows pointing to remaining phases of intermetallic compounds; double-headed arrows and σ indicating tensile testing direction and tensile stress, respectively)

0.4Fe + 0.2Sc alloys. Figure 10a shows the fracture of 0.4Fe alloy. In the white oval, there are many microcracks in β phase. These microcracks are the crack initiation sites. The white arrows point to the remaining Fe-rich intermetallic compounds on the fracture surface. Figure 10b shows the fracture of 0.2Fe + 0.4Sc alloy. The Sc-rich intermetallic compounds in this alloy are small in both size and amount. There is a smaller amount of Sc-rich intermetallic compounds remaining on the fracture surface (white arrows) as compared to the other alloys. This is a reason why there were fewer initiation sites. Figure 10c

shows the result from the 0.4Fe + 0.4Sc alloy. The Fe-rich intermetallic compound (β phase) and Sc-rich intermetallic compounds in this alloy are bigger than those in 0.2Fe + 0.4Sc alloy. There are microcracks inside β phase and Sc-rich intermetallic compounds, as shown in the white ovals. There are more Fe-rich and Sc-rich intermetallic compounds remaining on the fracture (white arrows) than in 0.2Fe + 0.4Sc alloy. Thus, 0.4Fe and 0.2Fe + 0.4Sc alloys have many crack initiation sites. The results confirm that Fe-rich and Sc-rich intermetallic compounds should be the crack initiation sites.

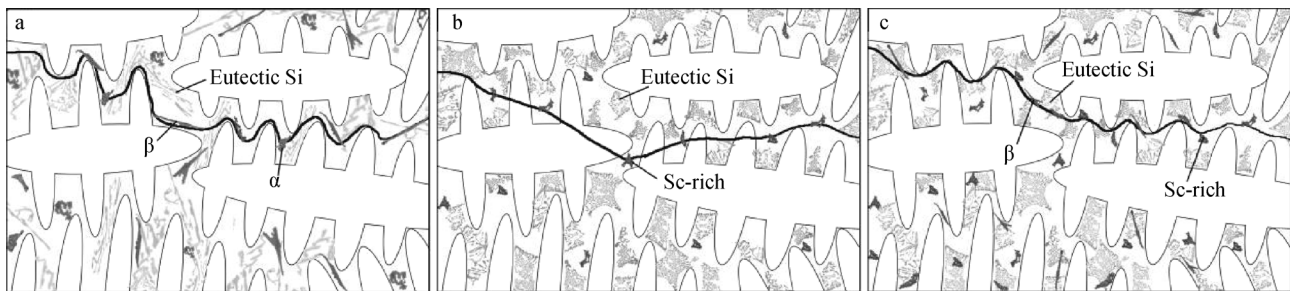


Fig. 11 Schematic of proposed fracture patterns of **a** Sc-free alloy, **b** low-Fe alloy with Sc and **c** high-Fe alloy with Sc (white areas being α -aluminum, black particles being eutectic silicon, gray particles being Fe-rich intermetallic compounds and Sc-rich intermetallic compounds and black line being fracture pattern)

Figure 11 shows a schematic of proposed fracture paths to help explain how fracture occurs. White areas are the α -aluminum, gray particles are the eutectic silicon, black particles are the Fe-rich and Sc-rich intermetallic compounds, and black line is the fracture path. In Sc-free alloy (Fig. 11a), the eutectic silicon and Fe-rich intermetallic compounds (α phase and β phase) have a large size and a sharp edge. The fracture starts from Fe-rich intermetallic compounds and eutectic silicon. The fracture path of Sc-free alloy runs along eutectic silicon and Fe-rich intermetallic compounds along the edges of dendrite arms. For the low-Fe alloy with Sc (Fig. 11b), the morphology of eutectic silicon is small and fibrous. The size of Sc-rich intermetallic compounds is small, and the amount is low. The fracture occurs difficultly. The α -primary dendrite has time to elongate before breaking. The fracture runs through some dendrites. The fracture path of low-Fe alloy with Sc runs through both dendrite and interdendritic eutectic. For high-Fe alloy with Sc (Fig. 11c), the morphology of eutectic silicon is small and fibrous. The Fe-rich intermetallic compound (β phase) and Sc-rich intermetallic compounds are bigger in size and larger in amount than those in low-Fe alloy with Sc. Crack initiation occurs from these intermetallic compounds. The fracture path of the high-Fe alloy with Sc can run through the group of eutectic silicon. The larger amount of intermetallic compounds indicates that it is easier for crack initiation.

4 Conclusion

The effect of scandium on mechanical properties of Al-7Si-0.3Mg was studied. In squeeze casting of Al-7Si-0.3Mg, the addition of a small amount of Sc changes Fe-rich intermetallic compounds into Sc-rich intermetallic compounds. Sc-rich intermetallic compounds tend to be small in size and round in shape. At the same time, adding Sc changes the morphology of eutectic silicon to small and fibrous shape. At a low amount of iron (0.2 wt% Fe), the addition of a small amount of Sc increases the hardness,

yield strength and ultimate tensile strength while maintaining a good elongation. A small amount of small and round Sc-rich intermetallic compounds forms, and the eutectic silicon becomes small and fibrous. These changes help increase the tensile strength of this alloy while maintaining a good elongation. At a high amount of iron (0.4 wt% Fe), the addition of a small amount of Sc increases the hardness, yield strength and ultimate tensile strength while decreasing the elongation slightly. A high amount of Sc-rich intermetallic compounds forms in this alloy, and they act as crack initiation sites to reduce the elongation of these alloys slightly. The elongation of Al-7Si-0.3Mg is affected by the distribution, size, shape of intermetallic compounds and eutectic silicon. The intermetallic compounds can act as crack initiation sites. Increasing the amount of intermetallic compounds reduces the elongation.

Acknowledgements This work was financially supported by the Royal Golden Jubilee Ph.D. Program (No. PHD/0285/2552) and the King Mongkut's University of Technology Thonburi, National Metal and Materials Technology Center (No. MT-B-58-MET-07-265-1).

References

- [1] Lu L, Dahle AK. Iron-rich intermetallic phases and their role in casting defect formation in hypoeutectic Al-Si alloys. *Metall Mater Trans A*. 2005;36(13):819.
- [2] Gorny A, Manickaraj J, Cai Z, Shankar S. Evolution of Fe based intermetallic phases in Al-Si hypoeutectic casting alloys: influence of the Si and Fe concentrations, and solidification rate. *J Alloy Compd*. 2013;577:103.
- [3] Han YS, Choi JO, Choi CO, McCartney DG. Intermetallic phase formation in directionally solidified Al-Si-Fe alloy. *Met Mater Int*. 2004;10(1):27.
- [4] Tang SK, Sriharan T. Morphology of β -AlFeSi intermetallic in Al-7Si alloy castings. *Mater Sci Technol*. 1998;14(8):738.
- [5] Sweet L, Zhu SM, Gao SX, Taylor JA, Easton MA. The effect of iron content on the iron-containing intermetallic phases in a cast 6060 aluminum alloy. *Metall Mater Trans A*. 2011;42(7):1737.
- [6] Taylor JA. Iron-containing intermetallic phases in Al-Si based casting alloys. *Proced Mater Sci*. 2012;1:19.

- [7] Murali S, Raman KS, Murthy KSS. The formation of β -FeSiAl₅ and Be–Fe phases in Al–7Si–0.3 Mg alloy containing Be. *Mater Sci Eng A*. 1995;190(1):165.
- [8] Puncrobutr C, Lee PD, Kareh KM, Connolley T, Fife JL, Phillion AB. Influence of Fe-rich intermetallics on solidification defects in Al–Si–Cu alloys. *Acta Mater*. 2014;68:42.
- [9] Ma Z, Samuel AM, Samuel FH, Doty HW, Valtierra S. A study of tensile properties in Al–Si–Cu and Al–Si–Mg alloys: effect of β -iron intermetallics and porosity. *Mater Sci Eng A*. 2008;490(1):36.
- [10] Kim HY, Han SW, Lee HM. The influence of Mn and Cr on the tensile properties of A356–0.20 Fe alloy. *Mater Lett*. 2006;60(15):1880.
- [11] Shabestari SG. The effect of iron and manganese on the formation of intermetallic compounds in aluminum–silicon alloys. *Mater Sci Eng A*. 2004;383(2):289.
- [12] Gustafsson G, Thorvaldsson T, Dunlop GL. The influence of Fe and Cr on the microstructure of cast Al–Si–Mg alloys. *Metall Trans A*. 1986;17(1):45.
- [13] Tan YH, Lee SL, Lin YL. Effects of Be and Fe additions on the microstructure and mechanical properties of A357.0 alloys. *Metall Mater Trans A*. 1995;26(5):1195.
- [14] Hwang JY, Doty HW, Kaufman MJ. The effects of Mn additions on the microstructure and mechanical properties of Al–Si–Cu casting alloys. *Mater Sci Eng A*. 2008;488(1):496.
- [15] Seifeddine S, Johansson S, Svensson IL. The influence of cooling rate and manganese content on the β -Al₅FeSi phase formation and mechanical properties of Al–Si-based alloys. *Mater Sci Eng A*. 2008;490(1):385.
- [16] McDonald SD, Dahle AK, Taylor JA, StJohn DH. Eutectic grains in unmodified and strontium-modified hypoeutectic aluminum–silicon alloys. *Metall Mater Trans A*. 2004;35(6):1829.
- [17] Dahle AK, Nogita K, McDonald SD, Zindel JW, Hogan LM. Eutectic nucleation and growth in hypoeutectic Al–Si alloys at different strontium levels. *Metall Mater Trans A*. 2001;32(4):949.
- [18] Jenkinson DC, Hogan LM. The modification of aluminium–silicon alloys with strontium. *J Cryst Growth*. 1975;28(2):171.
- [19] Mohanty PS, Gruzleski JE. Mechanism of grain refinement in aluminium. *Acta Metall Mater*. 1995;43(5):2001.
- [20] Johnsson M, Backerud L, Sigworth GK. Study of the mechanism of grain refinement of aluminum after additions of Ti- and B-containing master alloys. *Metall Trans A*. 1993;24(2):481.
- [21] Sun Y, Song M, He Y. Effects of Sc content on the mechanical properties of Al–Sc alloys. *Rare Met*. 2010;29(5):451.
- [22] Li W, Pan Q, Zou L, Liang W, He Y, Liu J. Effects of minor Sc on the microstructure and mechanical properties of Al–Zn–Mg–Cu–Zr based alloys. *Rare Met*. 2009;28(1):102.
- [23] Patakham U, Kajornchaiyakul J, Limmaneevichitr C. Grain refinement mechanism in an Al–Si–Mg alloy with scandium. *J Alloy Compd*. 2012;542:177.
- [24] Prukkanon W, Srisukhumbowornchai N, Limmaneevichitr C. Modification of hypoeutectic Al–Si alloys with scandium. *J Alloy Compd*. 2009;477(1):454.
- [25] Patakham U, Kajornchaiyakul J, Limmaneevichitr C. Modification mechanism of eutectic silicon in Al–6Si–0.3Mg alloy with scandium. *J Alloy Compd*. 2013;575:273.
- [26] Pandee P, Gourlay CM, Belyakov SA, Ozaki R, Yasuda H, Limmaneevichitr C. Eutectic morphology of Al–7Si–0.3Mg alloys with scandium additions. *Metall Mater Trans A*. 2014;45(10):4549.
- [27] Patakham U, Limmaneevichitr C. Effects of iron on intermetallic compound formation in scandium modified Al–Si–Mg Alloys. *J Alloy Compd*. 2014;616:198.
- [28] Chanyathunyaraj K, Patakham U, Kou S, Limmaneevichitr C. Microstructural evolution of iron-rich intermetallic compounds in scandium modified Al–7Si–0.3Mg alloys. *J Alloy Compd*. 2017;692:865.
- [29] Ghomashchi MR, Vikhrov A. Squeeze casting: an overview. *J Mater Process Technol*. 2000;101(1):1.
- [30] Ye H. An overview of the development of Al–Si-alloy based material for engine applications. *J Mater Eng Perform*. 2003;12(3):288.
- [31] Tzeng YC, Wu CT, Bor HY, Horng JL, Tsai ML, Lee SL. Effects of scandium addition on iron-bearing phases and tensile properties of Al–7Si–0.6Mg alloys. *Mater Sci Eng A*. 2014;593:103.
- [32] Lin B, Zhang WW, Lou ZH, Zhang DT, Li YY. Comparative study on microstructures and mechanical properties of the heat-treated Al–5.0Cu–0.6Mn–xFe alloys prepared by gravity die casting and squeeze casting. *Mater Des*. 2014;59:10.
- [33] Rokhlin LL, Bochvar NR, Rybal'chenko OV, Tarytina IE, Sukhanov AV. Phase equilibria in aluminum-rich Al–Sc–Si alloys during solidification. *Russ Metall (Metally)*. 2012;7:606.
- [34] Zhang F, Qin A, Liu S, Wang J, Du Y. Phase equilibria and solidification characteristics of the Al–Sc–Si alloys. *J Mater Sci*. 2016;51(3):1644.
- [35] Gruzleski JE, Closset BM. *The Treatment of Liquid Aluminum–Silicon Alloys*. Schaumburg: Amer Foundry Society; 1990. 75.
- [36] Closset B, Gruzleski JE. Structure and properties of hypoeutectic Al–Si–Mg alloys modified with pure strontium. *Metall Trans A*. 1982;13(6):945.
- [37] Tsai YC, Chou CY, Lee SL, Lin CK, Lin JC, Lim S. Effect of trace La addition on the microstructures and mechanical properties of A356 (Al–7Si–0.35Mg) aluminum alloys. *J Alloy Compd*. 2009;487(1):157.
- [38] Jiang WM, Fan ZT, Liu DJ. Microstructure, tensile properties and fractography of A356 alloy under as-cast and T6 obtained with expendable pattern shell casting process. *Trans Nonferrous Metals Soc China*. 2012;22:s7.